




RESEARCH PAPER

In vitro and *in vivo* characterization of the bifunctional μ and δ opioid receptor ligand UFP-505

Correspondence Professor D. G. Lambert, Department of Cardiovascular Sciences, University of Leicester, Division of Anaesthesia, Critical Care and Pain Management, Leicester Royal Infirmary, Leicester, UK. E-mail: dgl3@le.ac.uk

Received 27 February 2017; **Revised** 21 February 2018; **Accepted** 22 February 2018

N Dietis^{1,*} , H Niwa^{1,*}, R Tose^{1,*}, J McDonald¹, V Ruggieri², M Filafarro³, G Vitale⁴, L Micheli⁵, C Ghelardini⁵, S Salvadori⁶, G Calo⁶ , R Guerrini⁷, D J Rowbotham⁸ and D G Lambert¹ 

¹Department of Cardiovascular Sciences, University of Leicester, Division of Anaesthesia, Critical Care and Pain Management, Leicester Royal Infirmary, Leicester, UK, ²Department of Oncology Haematology and Respiratory Diseases, University of Modena and Reggio Emilia, Modena, Italy, ³Department of Biomedical, Metabolic and Neuro-Sciences, University of Modena and Reggio Emilia, Modena, Italy, ⁴Section of Pharmacology, Department of Life Sciences, University of Modena and Reggio Emilia, Modena, Italy, ⁵Department of Preclinical and Clinical Pharmacology, University of Florence, Florence, Italy, ⁶Department of Experimental and Clinical Medicine, Section of Pharmacology, University of Ferrara, Ferrara, Italy, ⁷Department of Pharmaceutical Sciences, University of Ferrara, Ferrara, Italy, and ⁸Department of Health Sciences, University of Leicester, Division of Anaesthesia, Critical Care and Pain Management, Leicester Royal Infirmary, Leicester, UK

*Present address for N.D., Medical School, University of Cyprus, 1 University Avenue, Aglantzia 2109, Nicosia, Cyprus. For H.N. and R.T., Department of Anesthesiology, University of Hirosaki, Hirosaki, Japan.

BACKGROUND AND PURPOSE

Targeting more than one opioid receptor type simultaneously may have analgesic advantages in reducing side-effects. We have evaluated the mixed μ opioid receptor agonist/ δ opioid receptor antagonist UFP-505 *in vitro* and *in vivo*.

EXPERIMENTAL APPROACH

We measured receptor density and function in single μ , δ and μ / δ receptor double expression systems. GTP γ ³⁵S binding, cAMP formation and arrestin recruitment were measured. Antinociceptive activity was measured *in vivo* using tail withdrawal and paw pressure tests following acute and chronic treatment. In some experiments, we collected tissues to measure receptor densities.

KEY RESULTS

UFP-505 bound to μ receptors with full agonist activity and to δ receptors as a low efficacy partial agonist At μ , but not δ receptors, UFP-505 binding recruited arrestin. Unlike morphine, UFP-505 treatment internalized μ receptors and there was some evidence for internalization of δ receptors. Similar data were obtained in a μ / δ receptor double expression system. In rats, acute UFP-505 or morphine, injected intrathecally, was antinociceptive. In tissues harvested from these experiments, μ and δ receptor density was decreased after UFP-505 but not morphine treatment, in agreement with *in vitro* data. Both morphine and UFP-505 induced significant tolerance.

CONCLUSIONS AND IMPLICATIONS

In this study, UFP-505 behaved as a full agonist at μ receptors with variable activity at δ receptors. This bifunctional compound was antinociceptive in rats after intrathecal administration. In this model, dual targeting provided no advantages in terms of tolerance liability.

LINKED ARTICLES

This article is part of a themed section on Emerging Areas of Opioid Pharmacology. To view the other articles in this section visit <http://onlinelibrary.wiley.com/doi/10.1111/bph.v175.14/issuetoc>

Abbreviations

DAMGO, [D-Ala², NMe-Phe⁴, Gly-ol⁵]-enkephalin; DPDPE, [D-Pen², D-Pen⁵]-enkephalin; UFP-505, H-Dmt-Tic-Gly-NH-Bzl; DPN, diprenorphine; EM1, endomorphin-1; GTPγ³⁵S, guanosine 5'-[γ-³⁵S-thio]triphosphate; NOP, nociceptin/orphanin FQ receptor

Introduction

Opioids have been the main treatment option for pain for centuries, but their use is associated with a number of troublesome side effects, including respiratory depression, constipation, immune suppression, physical dependence and tolerance (Dietis *et al.*, 2011; Sehgal *et al.*, 2013). Analgesic tolerance is a long-term process, which is distinct to the rapid process of desensitization that arises from chronic administration of opioids (Dang and Christie, 2012). When analgesic tolerance occurs, the patient requires increasingly higher doses of the drug in order to achieve adequate analgesia. As these higher doses result in increased side effects, including tolerance itself, it is easy to appreciate that tolerance drives an inevitable vicious clinical circle of increasing doses and increased side effects, which is the end result of chronic opioid use (Dietis *et al.*, 2009). Clinically, an increase in opioid analgesia can be achieved by switching opioid or adding an adjuvant, and the World Health Organization analgesic ladder describes this from a practical standpoint. However, a short-term increase in analgesia does not attenuate the development of tolerance, and therefore, a reduction in the degree of analgesia achieved is inevitable. Therefore, reducing the propensity for tolerance in novel opioids is an efficient strategy for providing adequate analgesia without detrimental dose-escalation.

Opioid receptors are members of a large family comprising the μ , δ , κ and the 'opioid-like' **nociceptin/orphanin FQ receptor (NOP)**; Lambert, 2008; Dietis *et al.*, 2011; Toll *et al.*, 2018). Almost all clinically available (and pharmaceutical developed) opioid analgesics target mainly the μ receptors, although there is current evidence for constitutive interactions among receptor subtypes (dimerization) that might change the way we think about the drug–target relationship of opioids (Gupta *et al.*, 2006). With relevance to our study, the most functionally important interaction of opioid receptors occurs between the μ and δ receptors (Law *et al.*, 2005). Gomes *et al.* (2000) provided evidence that μ - δ receptor dimers possess functional and ligand binding synergy, whereas George *et al.* (2000) showed a distinct binding profile of opioid ligands at μ - δ receptor dimers. More interestingly, however, a number of earlier studies in rodents have shown that when δ receptors are blocked by an antagonist (Abdelhamid *et al.*, 1991; Hepburn *et al.*, 1997) or the gene is knocked out (Zhu *et al.*, 1999) or knocked down (Kest *et al.*, 1996), or the gene for the endogenous δ receptor agonist enkephalin is knocked out (Nitsche *et al.*, 2002), then tolerance to morphine is reduced.

From a drug development perspective, it is preferable to use a single molecule to simultaneously target the μ and δ receptors, rather than co-administering two separate drugs, both from a pharmacokinetic point of view and reduced drug interactions. For this purpose, two chemical types of opioids

can be considered: bifunctional opioids (e.g. opioids that have two distinct binding properties) and bivalent opioids (e.g. opioids that possess two distinct pharmacophores in their structure) (Dietis *et al.*, 2009). Although these two types of 'dual' opioids have been well described in the literature during the last decade, their differentiation in terms of advances in chemical design or molecular efficacy is not yet clear.

Our group has used the bifunctional opioid H-Dmt-Tic-Gly-NH-Bzl (UFP-505) as a prototype μ receptor agonist and δ receptor antagonist (Balboni *et al.*, 2010; Dietis *et al.*, 2012) and hypothesized that this opioid ligand will produce antinociceptive actions *in vivo* with reduced analgesic tolerance liability. Here, we present our data from relevant *in vivo* assays on the tolerance, as well as new data on this ligand's effects on opioid receptor density and trafficking from assays *in vitro*, at recombinant μ and δ receptors and at μ/δ double expression receptor systems, and *ex vivo*, using rat tissues.

Methods

Additional information for the materials used can be found in the Supporting Information.

Cell culture

CHO cells stably expressing a single type of human opioid receptor (μ receptors, hMOP and δ receptors, hDOP) and cells with high expression of human δ receptors (CHO_{hDOP/high}) were grown as described previously (Dietis *et al.*, 2012). Stock cultures were supplemented with 200 $\mu\text{g}\cdot\text{mL}^{-1}$ geneticin (G418), for CHO_{hMOP}, CHO_{hDOP} and CHO_{hDOP/high} cells, and with additional 200 $\mu\text{g}\cdot\text{mL}^{-1}$ hygromycin B for the novel CHO_{hMOP/hDOP} cell line (see below). Cell cultures were kept at 37°C in 5% CO₂/humidified air and subcultured as required using trypsin/EDTA. Cells were used for experimentation as they approached confluence and were selection agent free.

Novel cell line stably expressing human μ and δ receptors

A novel CHO cell line stably expressing the human μ and δ receptors (CHO_{hMOP/hDOP}) was produced by transfecting geneticin-resistant CHO_{hMOP} cells with human δ receptor cDNA in a hygromycin B-selectable vector (pcDNA3.1Hygro(+)/OPRD1; S&T Missouri University, USA) and selected with 800 $\mu\text{g}\cdot\text{mL}^{-1}$ hygromycin B and 500 $\mu\text{g}\cdot\text{mL}^{-1}$ geneticin (GIBCO, UK). Initially, the transfection of human δ receptors in CHO_{hMOP} cells produced a polyclonal mixture which was further subcloned producing a final number of 30 CHO_{hMOP/hDOP} clones. To narrow the selection for the appropriate monoclonal cell batch, all clones were screened

by qRT-PCR and their μ and δ receptor mRNA expression levels were determined. The top three clones that showed the highest transfection efficiency were used in radioligand binding assays to determine receptor protein expression. One clone was selected for use, and binding data are described in the Results section. Cell culturing of CHO_{hMOP/hDOP} cells was as described above with double selection pressure.

Saturation-binding assay to determine receptor density

Membrane protein from CHO cells (70–100 μ g; prepared as described in the Supporting Information) was incubated in 0.5 mL volume of 50 mM Tris, 0.5% BSA, with a variety of peptidase inhibitors (amastatin, **bestatin**, **captopril** and phosphoramidon) at 10 μ M and various concentrations of radioligand [³H]-diprenorphine ([³H]-DPN) for 1 h at room temperature. Tritiated DAMGO ([³H]-DAMGO) and tritiated **naltrindole** ([³H]-NT) was used for labelling μ and δ receptors, respectively, in saturation binding assays as appropriate. In some experiments (as noted in Results), full saturation analysis was performed, and in others, a saturating radioligand concentration was used. Non-specific binding (NSB) was defined in the presence of 10 μ M **naloxone**. Reactions were terminated and bound/free radioactivity were separated by vacuum filtration through polyethylenimine-soaked (0.5%) Whatman GF/B filters, using a Brandel harvester. Bound radioactivity was determined after 8 h extraction in ScintisafeGel (Wallac, Loughborough, UK) using liquid scintillation spectroscopy.

Displacement binding assay to determine ligand selectivity and binding affinity

Membrane protein (70–100 μ g) was incubated, as in the saturation assays, but containing ~1 nM [³H]-DPN and varying concentrations (1 pM to 10 μ M) of a range of displacer ligands. NSB was defined in the presence of 10 μ M naloxone. Assay incubation time, reaction termination and bound radioactivity were the same as in the saturation assay.

GTP γ ³⁵S assay to determine ligand functional activity

Membrane protein (70–100 μ g) was incubated in 0.5 mL volume of 50 mM Tris, 0.2 mM EGTA, 1 mM MgCl₂·6H₂O, 100 mM NaCl, pH 7.4 supplemented with 0.1% BSA, 0.15 mM bacitracin, GDP (33 μ M) and ~150 pM GTP γ ³⁵S with gentle shaking for 1 h at 30°C. NSB was determined in the presence of non-radiolabelled 10 μ M GTP γ S. Reactions were terminated by vacuum filtration through dry Whatman GF/B filters, using a Brandel harvester. Bound radioactivity was determined as in the saturation assays. **Endomorphin-1 (EM1)**, **[D-Pen²,D-Pen⁵]-enkephalin (DPDPE)** or UFP-505 were included where appropriate at various concentrations and combinations as described in the Results section.

Inhibition of forskolin-stimulated cAMP formation

CHO whole-cell suspensions were incubated in 300 μ L Krebs/HEPES buffer (143 mM NaCl, 4.7 mM KCl, 2.6 mM CaCl₂,

1.2 mM MgSO₄, 1.2 mM KH₂PO₄, 12 mM glucose and 10 mM HEPES, pH to 7.4) containing 0.5% BSA, 1 mM IBMX, 1 μ M forskolin and 10 μ M of EM1, DPDPE and UFP-505. Reactions were incubated for 15 min at 37°C, with gentle shaking, terminated by addition of 20 μ L 10 M HCl, neutralized by addition of 20 μ L 10 M NaOH and buffered to pH 7.4 by addition of 200 μ L 1 M Tris-HCl. Cellular debris was cleared by centrifugation and the resulting supernatants assayed for cAMP formation, against cAMP standards, in a competitive binding assay with [³H] cAMP using a binding protein extracted from bovine adrenal glands, as described previously (Kitayama *et al.*, 2007). Bound and free radioactivity were separated by the addition of 250 μ L of charcoal mixture (250 mg charcoal, 100 mg BSA per 25 mL solution, 50 mM Tris-HCl and 4 mM EDTA buffer at pH 7.4). Each tube was allowed to stand for 1 min before centrifugation at 12000 \times g in a Sarstedt microfuge at room temperature. The supernatant (200 μ L) was taken and mixed with 1 mL of Optiphase Hi-Safe scintillation liquid, and radioactivity was counted using liquid scintillation spectroscopy.

Receptor internalization and receptor desensitization assays

For the internalization study, cells (grown in large T175 flasks) were incubated with appropriate concentration of a given ligand in 20 mL of fresh culture medium for an appropriate time according to the experiment and as described in the Results section. Adherent cells were then washed three times at 4°C with harvest buffer (containing 0.9% saline, 0.02% EDTA, 10 mM HEPES, pH of 7.4) to remove any receptor-bound ligand, before harvesting. Membranes were prepared as previously described (Dietis *et al.*, 2012), washing three times with buffer prior to three centrifugations at 1600 \times g and three centrifugations at 14000 \times g, with subsequent removal of supernatant and resuspension of the pellet, in order to ensure that all desensitizing ligand is washed off. Then a saturation binding assay was performed as described above. For receptor internalization, CHO_{hMOP} cells were treated with 10 μ M of **morphine**, EM1 or **fantanyl** and CHO_{hDOP} with 10 μ M DPDPE, as reference compounds with the maximum concentration used in these experiments, as well as with various concentrations of UFP-505 (1 nM–10 μ M) for CHO_{hMOP} or 10 μ M for CHO_{hDOP}. For the desensitization studies, cells were incubated for 1 h (chosen as the most appropriate for tolerance-related desensitization; based on Williams *et al.*, 2013) with an appropriate ligand at various concentrations (1 pM to 10 μ M), and membranes were prepared as in the internalization study. A GTP γ ³⁵S assay was then performed as described above.

Arrestin assay

The PathHunter® eXpress CHO-K1 pre-validated cell lines were used (DiscoverX, Birmingham, UK), expressing human μ or δ receptors and β -arrestin-2, supplied in an optimized cell culture medium. The assay measures binding of β -arrestin with the receptor of interest upon activation by an agonist. The assay was performed according to the manufacturer's instructions. Briefly, cells were thawed and plated in OCC medium in 96-well luminescence plates and allowed to recover for 48 h at 37°C. Agonists were added to each well and incubated for 90 min at 37°C. Detection reagents were

added and incubated with the cells for 60 min at room temperature. Chemiluminescence was measured using a standard 96-well plate luminometer.

Animals

All animal care and experimental procedures complied with the European Directive (EEC No. 86/609) and the Italian D. L. 27/01/1992, No.116, and were approved by the University of Florence or Modena Animal Subjects Review Board. Ethical guidelines for investigation of experimental pain in conscious animals were followed. Animal studies are reported in compliance with the ARRIVE guidelines (Kilkenny *et al.*, 2010; McGrath and Lilley, 2015).

Healthy male Wistar rats (strain code 003, albino, 200–250 g; Charles Rivers Laboratories, Wilmington, MA, USA) were used in the tail-flick (TF) antinociception assay and healthy male Sprague–Dawley rats (280–300 g; Harlan, Varese, Italy) were used in the paw pressure (PP) and rotarod assays. Before any surgical or experimental procedures, all animals were housed in groups of two to three under standard controlled conditions ($22 \pm 1^\circ\text{C}$, 12 h light/dark cycle) with food and water *ad libitum* for at least 5 days. Animal weight and visible behavioural changes were monitored prior, during and after each experiment. All animals were used at least 1-week after their arrival in the lab. After surgery and during experiments, all animals were housed singly.

Intrathecal surgery

We initially used an intrathecal (i.t.) catheterization protocol for animals used in the acute TF test, but it was not possible to retain the catheters on these animals for long-term exposure (data not shown). We therefore elected to use an alternative catheterization strategy for the rest of the tests used (rotarod and PP). Below, we describe both protocols used. For the TF test, animals were anaesthetized by i.p. ketamine and xylazine ($115 + 2 \text{ mg}\cdot\text{kg}^{-1}$; Farmaceutici Gellini, Aprilia, Italy, and Bayer, Milan, Italy), and a modification of the Storkson method of i.t. catheterization was applied (Storkson *et al.*, 1996) at the lumbar region of the spinal cord (between L5 and L6; Supporting Information Figure S1). After surgery, the correct catheter positioning was assessed by lidocaine administration ($15 \mu\text{L}$, $20 \text{ mg}\cdot\text{mL}^{-1}$, i.t.) followed by saline ($10 \mu\text{L}$, i.t.) and subsequent loss of motor control of the rear limbs within 15 s lasting for 20–30 min. One animal that did not pass this lidocaine test was excluded from the study.

The animals used in the rotarod and PP assays were anaesthetized with 2% isoflurane and the i.t. catheter was surgically implanted according to the method of Yaksh and Rudy (1976). Rats were shaved on the back of the neck and placed in the stereotaxic frame with the head securely held between ear bars. The skin over the nap of the neck was cleaned with ethyl alcohol and incised for 1 cm. The muscle on either side of the external occipital crest was detached and retracted to expose about 3–4 mm² of the atlanto-occipital membrane. The membrane was incised by a needle, which led to the escape of cerebrospinal fluid. The caudal edge of the cut was lifted, and about 7.0 cm of 28 g polyurethane catheter (0.36 mm outer diameter; 0.18 mm inner diameter; Alzet, USA) was gently inserted into the i.t. space in the midline, dorsal to the spinal cord until the lumbar enlargement. The exit end of the catheter was connected to 4.0 cm polyurethane (0.84 mm outer diameter; 0.36 mm inner diameter) and was taken out through the

skin, flushed with saline solution, sealed and securely fixed on the back of the head with a silk suture. The incision site in the skin was closed with polyamide sutures and the animals allowed to recover for 24 h before the study began. The evaluation of potential motor dysfunctions induced by the surgery was investigated using a rotarod test. Any animals displaying motor disabilities (approximately 10%) were excluded from the PP behavioural measurements.

Tail-flick test

Animals were submitted to the TF test (15 s cut-off time) prior to acute i.t. treatment of varying drug concentrations in order to determine their nociceptive threshold (basal latency) and after i.t. administration of drugs at times $T = 15, 30, 60, 90$ and 120 min to determine treatment latency. The control group animals were treated with sterile saline ($20 \mu\text{L}$) whereas the treatment group animals were treated with $10 \mu\text{L}$ (i.t.) of UFP-505 followed by administration of sterile saline ($10 \mu\text{L}$, i.t.). Morphine was also used as a reference compound in a separate animal group, in a protocol similar to the treatment group.

Rotarod test

The rotarod apparatus (Ugo Basile, Varese, Italy) was consisted of a base platform and a rotating rod with a diameter of 6 cm and a non-slippery surface. The rod, 36 cm in length, was placed at a height of 25 cm from the base and was divided into four equal sections by five disks. Thus, up to four rats were tested simultaneously on the apparatus, with a rod-rotating speed of 10 r.p.m. The integrity of motor coordination was assessed on the basis of the number of falls from the rod during 60 s in acute protocol and 120 s during the repeated one. The test was stopped after a maximum of six falls.

Paw pressure test

The mechanical nociceptive threshold in the rat was determined with the PP test (Ugo Basile, Varese, Italy), according to the method described by Leighton *et al.* (1988). A constantly increasing mechanical pressure was applied to the animal's paw, until occurrence of vocalization or withdrawal reflex, while the rats were lightly restrained. Vocalization or withdrawal reflex threshold levels were expressed in grams of the applied pressure. Animals with basal threshold below 40 g or above 75 g were excluded prior to treatment. Measurements were performed after acute i.t. injection of 0.3–30 nmol UFP-505 ($10 \mu\text{L}$). Antinociception was measured at 15, 30, 45 and 60 min after administration with a PP test. Chronic experiments (8 days) involved in i.t. daily injection of 10 nmol UFP-505 or 3 nmol morphine (in $10 \mu\text{L}$), and antinociception in PP (along with motor coordination using a rotarod; as described above) was evaluated every day at 30 min after administration. The cut-off threshold for treated animals in this assay was 150 g. Assessments of PP and motor coordination were performed independently of each other.

Tissue removal

Animals used in the TF test were killed by decapitation immediately after the end of each experiment, and their spinal cord tissue and cerebral cortex were isolated while on ice. Tissues were stored at -80°C and used later for membrane preparation as described above. Part of the tissues scheduled for later

PCR analysis were first treated with RNAlater® solution (AM7020, Applied Biosystems, USA) then stored at -20°C for 2 days and finally stored at -80°C for 3 days.

Data and statistical analysis

The data and statistical analysis comply with the recommendations on experimental design and analysis in pharmacology (Curtis *et al.*, 2015). All data are presented as mean \pm SEM from (n) experiments, as shown in the Figure and Table legends. Concentration–response curves were analysed by nonlinear regression using GraphPad Prism V5.0 software (San Diego, CA, USA). In saturation-binding assays, the receptor density (B_{max}) and radioligand equilibrium dissociation constant (pK_{d}) were obtained from saturation-binding isotherms and semi-log transformations of specific binding data. In displacement binding assays, 50% displacement of specific binding was corrected for the competing mass of radiolabel, and the pK_{i} values were obtained from displacement curves, and values were determined using nonlinear regression, corrected using the Cheng-Prusoff equation (Cheng and Prusoff, 1973) ($\log \{EC_{50}/(1 + [L]/K_{\text{d}})\}$), where EC_{50} is the effective concentration of the ligand that displaces 50% of the radioligand, $[L]$ the concentration of the radioligand used, and K_{d} the dissociation constant of the radioligand. pEC_{50} and E_{max} values in functional experiments were obtained from the sigmoidal curve with a variable slope. All statistical analysis was

performed using GraphPad Prism V5.0 software. Some data were analysed using 'Origin 9' software. Student's *t*-test and ANOVA with *post hoc* testing (Bonferroni) as required were used, as described in the Table and Figure legends (significance set at $P < 0.05$).

Nomenclature of targets and ligands

Key protein targets and ligands in this article are hyperlinked to corresponding entries in <http://www.guidetopharmacology.org>, the common portal for data from the IUPHAR/BPS Guide to PHARMACOLOGY (Harding *et al.*, 2018), and are permanently archived in the Concise Guide to PHARMACOLOGY 2017/18 (Alexander *et al.*, 2017).

Results

In vitro characterization of UFP-505

In part of the present study, we have used δ receptor-expressing cells with receptor density (Figure 1A left ~ 1.8 pmol mg-protein $^{-1}$), ~ 1.8 higher than the reported value in Dietsis *et al.* (2012). In membranes prepared from these high- δ receptor expressing cells, we found significant but low partial agonist activity for UFP-505 in a GTP $\gamma^{35}\text{S}$ assay (α 0.28 relative to DPDPE), as shown in Figure 1A right, indicating a partial agonist activity at δ receptors, at very high (non-physiological) receptor density. The potency of UFP-505

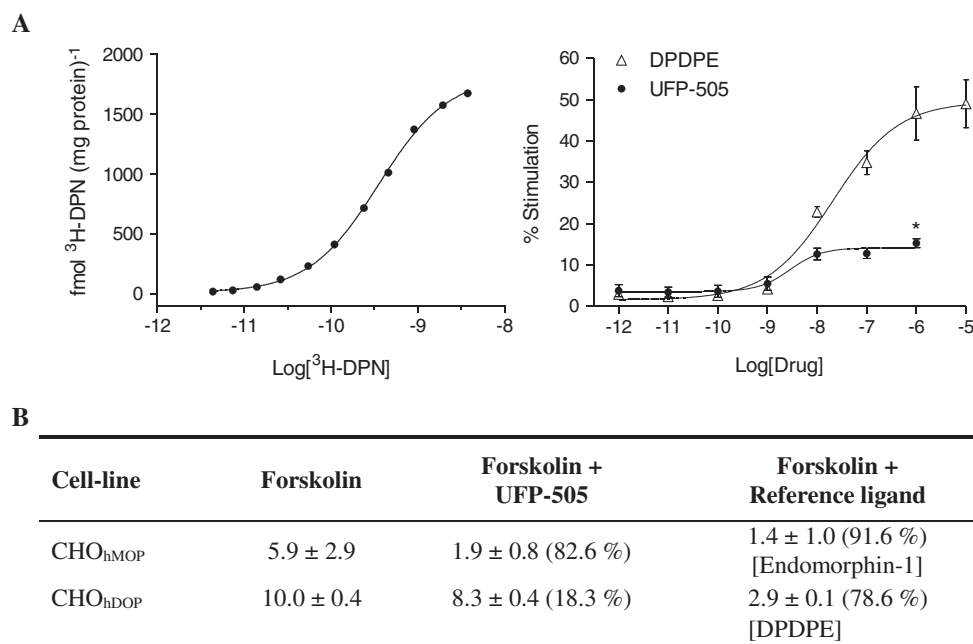


Figure 1

In vitro pharmacological characterization of UFP-505 in CHO cells. (A, left) Representative curve of a single saturation experiment (from 3 experiments to indicate density only) performed in CHO cells with high density of δ receptors. (A, right) G-protein stimulation by UFP-505 and DPDPE [(D-Pen 2,5)-enkephalin] in these high expressing cells ($n = 5$ per group). The maximum stimulation (E_{max}) achieved by UFP-505 binding was higher than basal levels (unstimulated), but less than that of DPDPE. * $P < 0.05$; Student's *t*-test (B) Effect of UFP-505 and reference agonists (DPDPE; 10 μM and EM1; 1 μM) on forskolin-stimulated cAMP formation in CHO_{hMOP} and CHO_{hDOP} (lower expression) cells. All data are presented as mean \pm SEM fold increase of basal stimulation ($n = 5-6$). Percentage inhibition of cAMP is shown in parenthesis. Both DPDPE and EM1 produced a significant inhibition compared to forskolin ($P < 0.05$, one-way ANOVA with Bonferroni correction).

(pEC_{50} ; 8.54 ± 0.28) was significantly higher than that of DPDPE (7.68 ± 0.20) in membranes from these cells.

Downstream from G-protein activation, the cAMP formation stimulated by forskolin, in CHO_{hMOP} cells was inhibited by both 1 μ M EM1 and 10 μ M UFP-505, as shown in Figure 1B. There was no significant difference between the inhibition of cAMP formation caused by EM1 and UFP-505, indicating that UFP-505 behaves as a full agonist in this downstream-amplified assay. In CHO_{hDOP} cells, 10 μ M DPDPE inhibited forskolin-stimulated cAMP formation as expected for a full agonist at δ receptors (Figure 1B). However, the addition of 10 μ M UFP-505 resulted in a small, but significant, inhibition of forskolin-stimulated cAMP (α 0.23 relative to DPDPE), again suggesting that UFP-505 behaves as a low-efficacy, partial agonist at δ receptors in this highly amplified assay. This is an important point in discussing the behaviour of the ligand *in vivo* at target 'sites' with higher expression.

In vitro receptor internalization

Next, we examined the effects of UFP-505 on opioid receptor turnover. Pretreatment of CHO_{hMOP} cells with 10 μ M UFP-505 induced a significant loss of surface μ receptors (62%) compared to the non-treated cells (Figure 2A). In the same assay, pretreatment with 10 μ M EM1 or fentanyl also induced significant μ receptor internalization (~50% and ~25%, respectively), whereas morphine was ineffective. To determine whether time of ligand pretreatment had an effect on the reduction of MOP receptor density, binding assays with saturating radioligand concentrations were performed after pretreatment of CHO_{hMOP} cells with 10 μ M UFP-505 for 1 and 24 h. Pretreatment with UFP-505 (control B_{max} 457 ± 86) for 24 h induced internalization of μ receptors (B_{max} 166 ± 15), comparable to the effects of pretreatment for 1 h (B_{max} 108 ± 23). These two B_{max} values were not different (one-way ANOVA with Bonferroni correction).

The decrease in μ receptor density induced by UFP-505 was concentration-dependent, as shown in Figure 2B. UFP-505 induced a significant internalization of μ receptors at 10 and 1 μ M compared to the control (untreated), with a pEC_{50} of 6.62. This is similar with the pEC_{50} produced from GTP γ^{35} S binding (6.37) but lower than the pK_i of UFP-505 binding (7.79) as shown in previously published data (Dietis *et al.*, 2012).

Interestingly, in CHO_{hDOP} cells (Figure 2C; B_{max} ~1000-fmol \cdot mg $^{-1}$ protein) where UFP-505 behaves as a low-efficacy partial agonist, 10 μ M of UFP-505 induced extensive internalization of δ receptors (~86%), as did the δ receptor full agonist DPDPE at 10 μ M (~80%). The unexpectedly extensive δ receptor internalization by UFP-505, based on its weak intrinsic activity, raised an initial concern that the reduction seen in this assay could be an artefact, possibly due to an incomplete wash-off of the desensitizing challenge. In order to exclude this possibility, full [3 H]-DPN saturation curves were produced from CHO_{hMOP} and CHO_{hDOP} cells pretreated with 10 μ M UFP-505 after wash off and the pK_d was calculated (Figure 3). Representative saturation curves are shown here, from a series of five independent experiments performed after pretreatment with 10 μ M fentanyl in CHO_{hMOP} cells (Figure 3B) and 10 μ M UFP-505 (Figure 3C). The pK_d of the curves produced were not different from the control (Figure 3G), confirming that the reduced radioligand binding

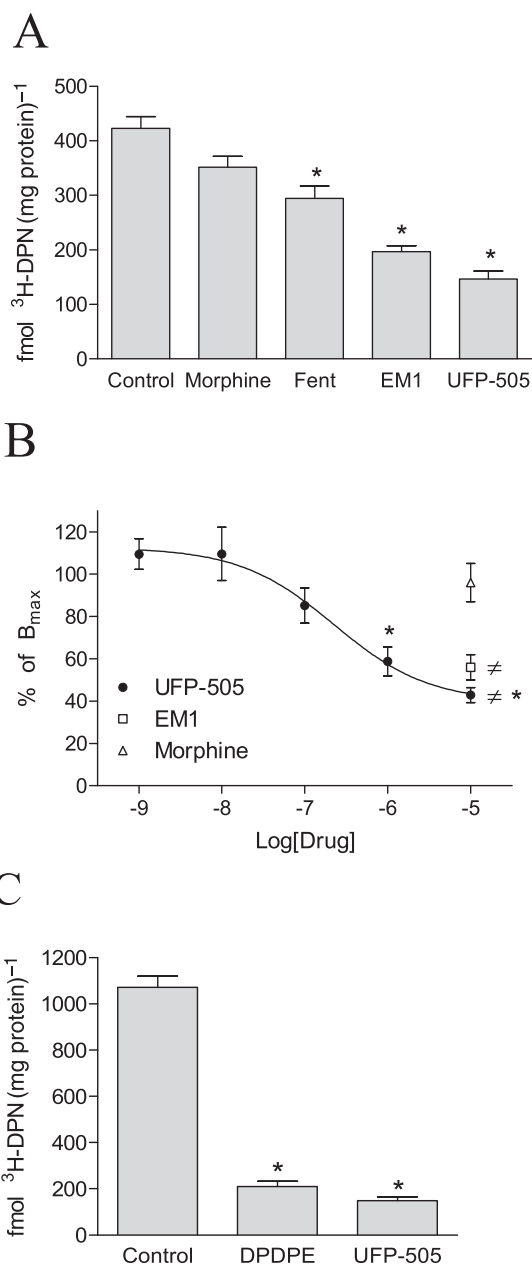


Figure 2

Opioid receptor internalization upon ligand binding. (A) μ receptor density (B_{max} ; fmol [3 H]-DPN \cdot mg $^{-1}$ protein) in CHO_{hMOP} cells pretreated for 1 h with various opioid ligands at 10 μ M as determined from binding assays with saturating radioligand concentrations. The B_{max} values after fentanyl (Fent), EM1 or UFP-505 were lower than control. * P < 0.05, significantly different from control; one-way ANOVA with Bonferroni test. (B) Internalization of μ receptors by UFP-505 is concentration-dependent. The pEC_{50} of internalization by UFP-505 was 6.62 ± 0.17 . Internalization by 10 μ M EM1 or 10 μ M morphine is also shown. Data are normalized to a control (untreated) B_{max} (set to 100%). * P < 0.05, significantly different from control; one-way ANOVA with Bonferroni test. $\neq P$ < 0.05, significantly different from 10 μ M morphine. (C) B_{max} of CHO_{hDOP} cells pretreated with 10 μ M UFP-505 or 10 μ M DPDPE for 1 h. Both treatments were equally effective. * P < 0.05, significantly different from control; one-way ANOVA with Bonferroni test. All data are means \pm SEM from $n = 5-7$.

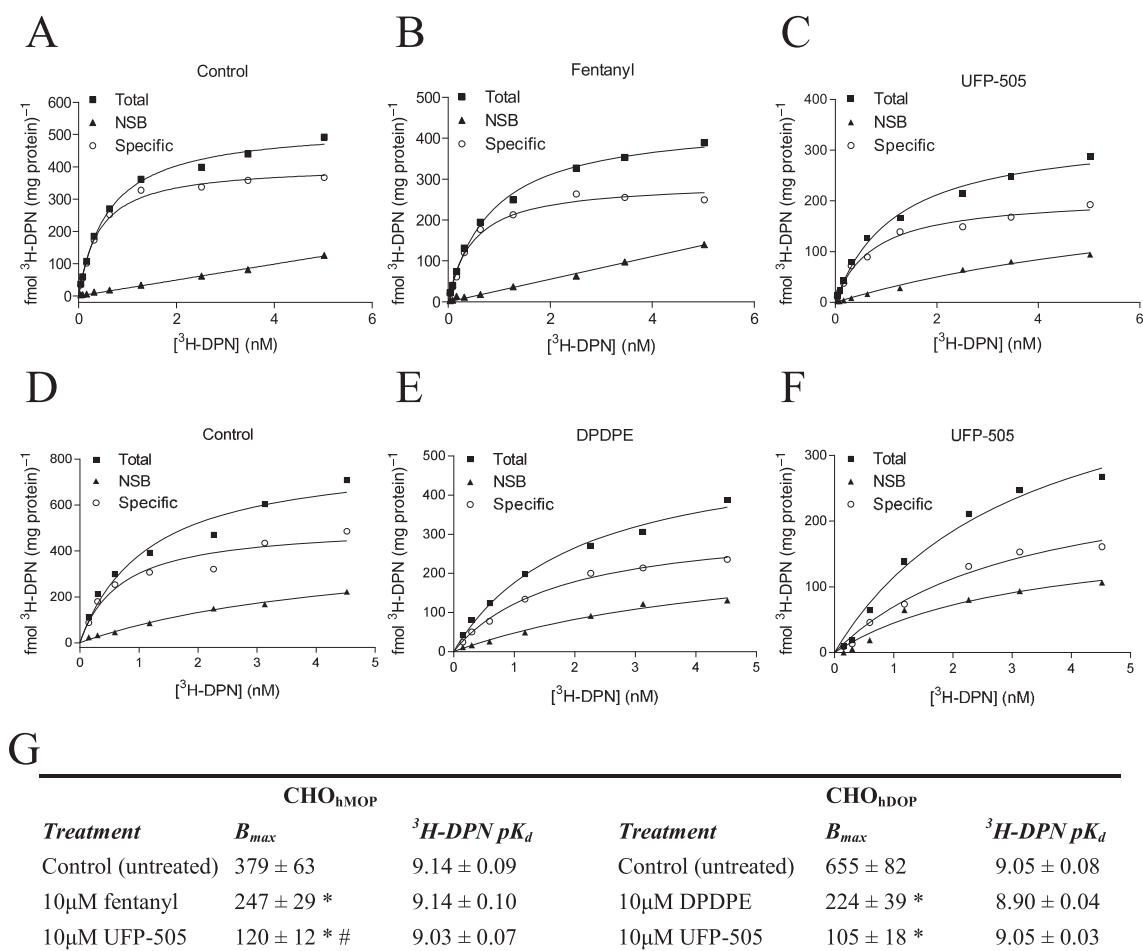


Figure 3

Full saturation curves and loss of cell surface receptors after treatment. Internalization of opioid receptors is presented as a reduction in the B_{max} (fmol [³H]-DPN·mg⁻¹ protein) in full saturation binding curves of CHO_{hMOP} cells (A–C) and CHO_{hDOP} cells (D–F) pretreated with 10 μM fentanyl, 10 μM DPDPE or 10 μM UFP-505. The lack of effect on the radioligand K_d confirms that the reduced B_{max} reflects genuine receptor internalization. Representative hyperbola are shown for μ or δ receptors from n = 5 experiments. Collective B_{max} and pK_d values are presented as mean ± SEM in (G). B_{max} values of treated cells were lower than their respective, untreated, controls. *P < 0.05, one-way ANOVA with Bonferroni test. The B_{max} of the UFP-505 treated cells was lower than that of the fentanyl-treated cells. #P < 0.05, one-way ANOVA with Bonferroni test. The same analysis has shown no significant differences in the pK_d between all groups.

shown in the internalization assays and interpreted as a reduction in the B_{max} is attributed solely to the internalization of the receptors and not to the presence of residual UFP-505 in the assay. Similarly, representative saturation curves from CHO_{hDOP} cells (from n = 5) after pretreatment with 10 μM DPDPE (Figure 3E) and 10 μM UFP-505 (Figure 3F) are also shown here, and the resulting pK_d of the curves from all pretreatment groups did not differ from the control.

Arrestin recruitment

As recruitment of arrestin is a critical part of the internalization process, we used the PathHunter® to compare arrestin recruitment with internalization. In CHO_{hMOP} cells, UFP-505 induced a concentration-dependent recruitment of β-arrestin to the μ receptor with a pEC₅₀ of 6.91 (Figure 4A), which was not significantly different to the pEC₅₀ of morphine (6.75). However, at 10 μM, morphine showed significantly lower E_{max} than UFP-505, EM1 and

fentanyl, whereas EM1 and fentanyl showed significantly higher E_{max} than UFP-505. For the δ receptors, although DPDPE produced a concentration-dependent recruitment of β-arrestin upon receptor activation, UFP-505 did not (Figure 4B). We do not know the receptor density of the cells used in this assay as they were provided ready-to-go by the assay manufacturer.

In vitro characterization of the double-expression system

All of our *in vitro* work so far had been with a single expression system, so in order to mimic the *in vivo* situation in a simple system, we produced CHO cells with double expression of μ and δ receptors. Our selected monoclonal CHO_{hMOP/hDOP} batch had a B_{max} of 672 ± 34 and 159 ± 32 fmol·mg⁻¹ (mean ± SEM) for the μ and δ receptors respectively, using tritiated naltrindole ([³H]-Nt) and DAMGO ([³H]-DAMGO) as δ receptor-selective and μ receptor-selective radioligands

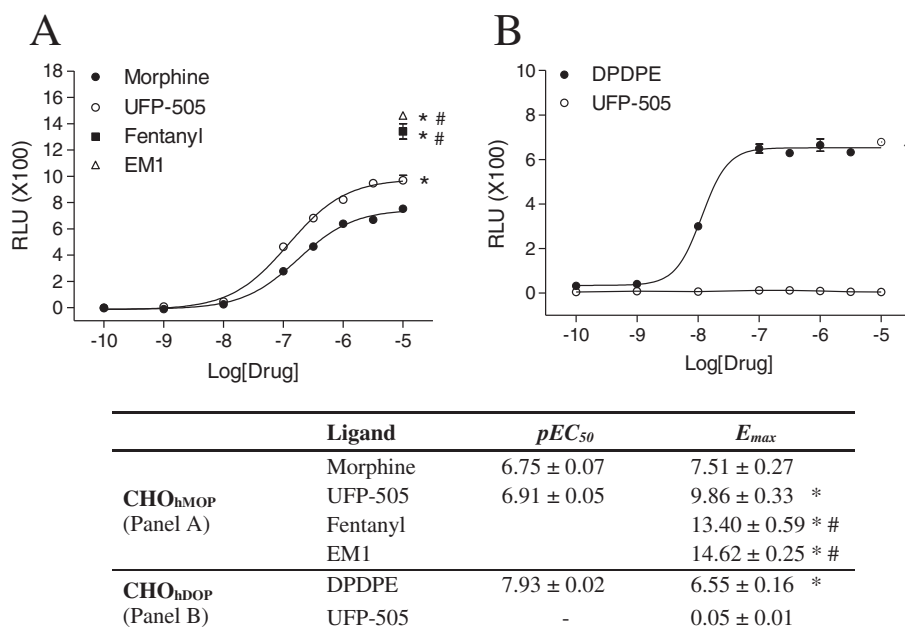


Figure 4

Concentration–response curves for β -arrestin recruitment in CHO_{hMOP} and CHO_{hDOP} cells for various agents. (A) Morphine, fentanyl, EM1 and UFP-505 in CHO_{hMOP}. (B) DPDPE and UFP-505 in CHO_{hDOP}. Response is presented as relative luminescence units (RLU). Data are mean \pm SEM of $n = 5$ experiments, performed in duplicate. In the CHO_{hMOP} cells, no significant difference was found between the EC_{50} values produced from the morphine and UFP-505 curves. Comparing the 10 μ M values among the different agents, the EM1, fentanyl and UFP-505 responses were all higher than that of morphine; * $P < 0.05$, whereas the EM1 and fentanyl responses were significantly higher than that of UFP-505; # $P < 0.05$. There was no difference between the EM1 and fentanyl responses. All analyses by one-way ANOVA with Bonferroni test. In the CHO_{hDOP} cells, the E_{max} values of DPDPE were significantly higher than that of UFP-505 (B; $P < 0.05$, Student's t -test).

in saturation binding assays. This gave a μ : δ receptor ratio of 4:1. In addition, full saturation curves with the non-selective ligand [³H]-DPN confirmed the overall expression levels of both types of opioid receptors to be 851 ± 45 fmol·mg⁻¹ as shown in Figure 5A; the numerical sum of individual μ receptors (672) and δ receptors (159), was 831 fmol·mg⁻¹, similar to that determined by [³H]-DPN.

Displacement binding assays showed an 'overall' DPN pK_d of 9.51 ± 0.19 for the double-expression CHO_{hMOP/hDOP} cells, similar to the pK_d produced for CHO_{hMOP} and CHO_{hDOP} cells (Dietis *et al.*, 2012). The binding of [³H]-DPN in CHO_{hMOP/hDOP} membranes was displaced in a concentration-dependent manner by UFP-505 and three reference ligands; EM1, naltrindole and morphine (Figure 5B). The 'overall' binding affinity (pK_i) of UFP-505 in CHO_{hMOP/hDOP} membranes was 7.70 ± 0.16 ($n = 5$), whereas the binding affinities for the respective reference ligands were to be 7.53 ± 0.10 (EM1), 7.87 ± 0.07 (naltrindole) and 7.75 ± 0.11 (morphine) respectively.

The capacity of UFP-505 to induce receptor internalization in the mixed μ and δ receptor population was then studied. UFP-505 induced ~62% opioid receptor internalization (μ and δ), significantly higher than morphine which did not induce significant internalization compared to control (Figure 5C). Pretreatment of DPDPE and EM1 produced ~27 and ~43% internalization respectively.

In the GTP γ ³⁵S assay, pretreatment of CHO_{hMOP/hDOP} cells with EM1 or UFP-505 produced a significant reduction in the

efficacy (E_{max}) of both ligands, without change in potency (pEC_{50}) (Figure 6). The next step from a simple double expression system was to examine behaviour *in vivo* in standard antinociceptive assays acutely and, after chronic treatment, to assess tolerance.

In vivo characterization of UFP-505

TF test. UFP-505 produced a time- and dose-dependent antinociceptive response (Figure 7). Treatment with 10 and 50 but not 1 and 3 nmol UFP-505 produced a significant response. Furthermore, animals treated with 50 nmol UFP-505 reached and retained the cut-off time from the first sampling point (15 min) throughout the study to 120 min (Figure 7A). Morphine, injected *i.t.*, in a dose of 10 nmol produced a similar antinociceptive profile to UFP-505 (10 nmol), which was not significantly different from 15 min until 90 min after injection. However, morphine antinociception was significantly reduced at 120 min after injection. An analysis of UFP-505 dose–response curves for latency at 120 min after administration and AUC (s·min) from Figure 7A are shown in Figure 7B. The pED_{50} values calculated for each curve were found to be very similar (8.20 ± 0.05 and 8.19 ± 0.18 respectively) and corresponded to ED_{50} values 6.27 and 6.38 nmol.

Paw pressure test. Acute administration of UFP-505 produced an antinociceptive response that peaked at 15–30 min. Compared to pretest values, there was a significant response

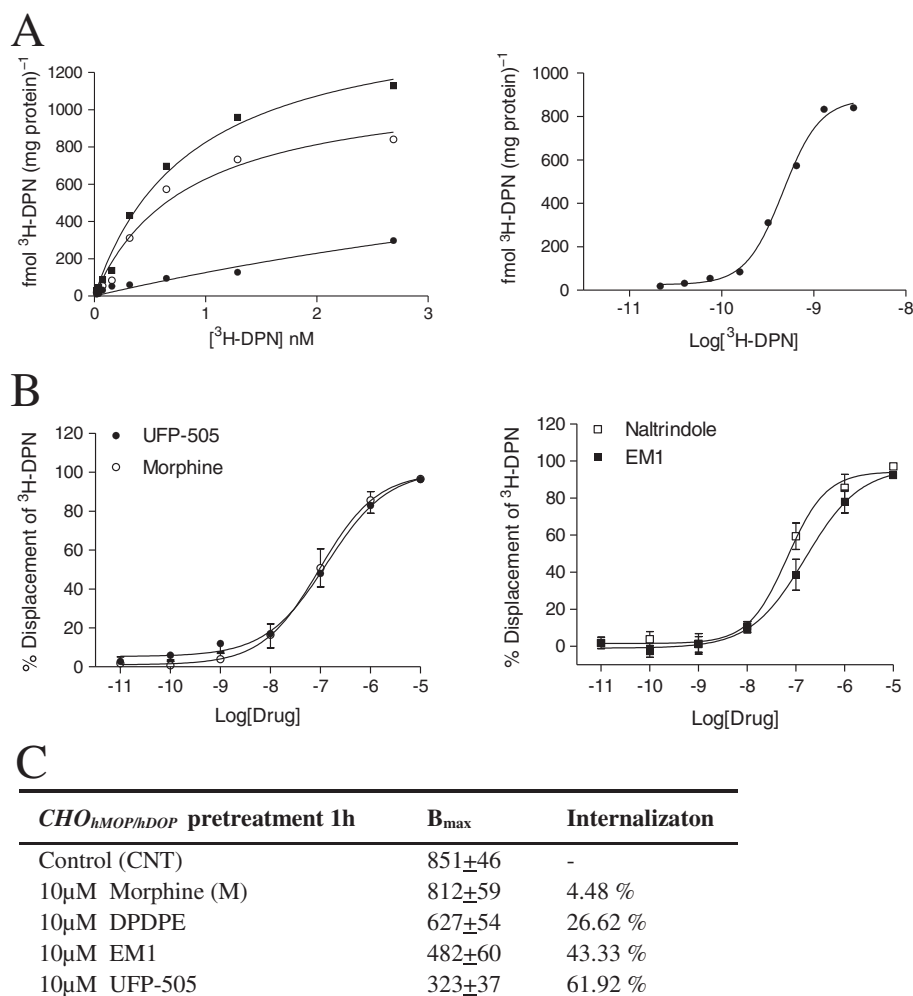


Figure 5

In vitro characterization of a *CHO*_{hMOP/hDOP} double-expression system. (A) Representative saturation binding curves (hyperbola; left and sigmoidal; right) performed on *CHO*_{hMOP/hDOP} cell membranes with increasing concentrations of [^3H]-DPN. NSB was measured in the presence of 10 μM naloxone. Single representative curves are presented here from a total of 3 experiments to indicate density only. The radioligand binding affinity as pK_d was 9.51 (K_d 30.9 nM). (B) Displacement of [^3H]-DPN by UFP-505 and reference ligands (naltrindole, morphine and EM1) at *CHO*_{hMOP/hDOP} cell membranes. Data are presented as mean \pm SEM ($n = 5$). Receptor binding affinities (pK_i) of ligands were calculated using the Cheng-Prusoff equation; 7.70 ± 0.16 (UFP-505), 7.75 ± 0.11 (morphine), 7.53 ± 0.10 (EM1) and 7.87 ± 0.07 (naltrindole). (C) Receptor density (B_{max} , $\text{fmol } [^3\text{H}]\text{-DPN}\cdot\text{mg}^{-1}$ protein) and percentage internalization of receptors in *CHO*_{hMOP/hDOP} cells pretreated for 1 h with various ligands, using a saturating concentration of [^3H]-DPN. Data are presented as mean \pm SEM values ($n = 3$). Receptor internalization is presented as a percentage of control.

to the 30 and 10 nmol doses at 15 and 30 min (Figure 8A). Based on the mechanical threshold at 15 min, a crude ED_{50} of ~ 9 nmol can be estimated, similar to that obtained in the TF assay. In Figure 8B, the effects of daily administration of 3 nmol morphine and 10 nmol UFP-505 are shown; based on previous data (Micheli *et al.*, 2015), this dose of morphine is equi-effective to 10 nmol UFP-505 in an acute setting. By days 6–7, animals were tolerant to both morphine and UFP-505. There were no differences in the time course for induction of tolerance between the two ligands.

Rotarod test. In both acute tests using the animals from the PP animal group, there were no significant effects on

performance at doses up to and including 10 nmol. At 30 nmol UFP-505, there was marked impairment of locomotor activity of the posterior paws; at the 15 min time point, the cut-off of six falls was reached (Table 1).

Ex vivo study of neuronal tissue from treated animals in the TF study

We had the opportunity to collect and analyse the neuronal tissue from the treated rats in order to assess the receptor turnover *in vivo* and to compare the produced data with our *in vitro* data. Membrane from lysates of rat neuronal tissue (cortex and spinal cord) of acutely treated animals (UFP-505, morphine and saline) was used for

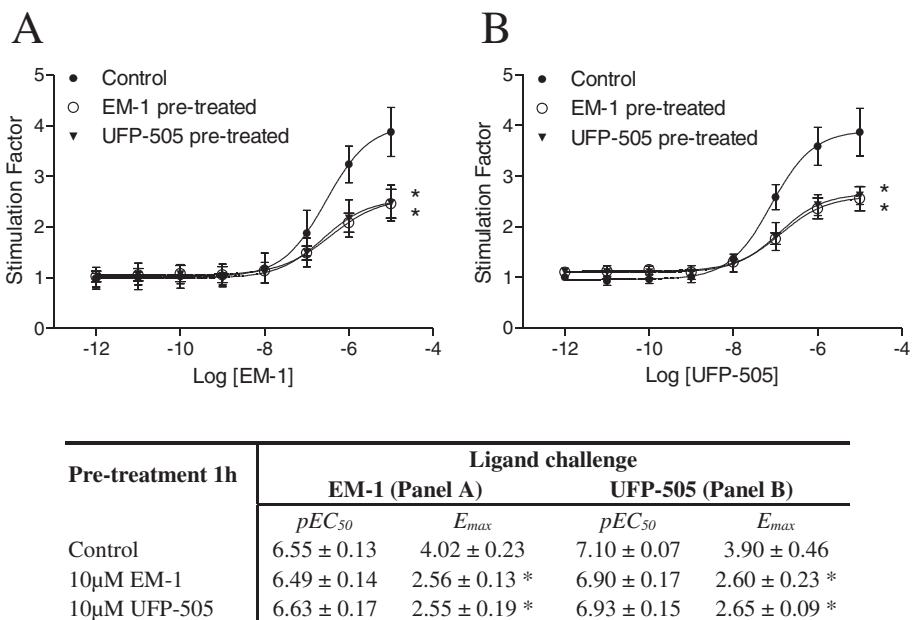


Figure 6

Receptor desensitization in CHO_{hMOP/hDOP} cells. Ligand-mediated GTPγ³⁵S binding measured in membranes prepared from CHO_{hMOP/hDOP} cells after pretreatment of CHO_{hMOP/hDOP} cells with 10 µM EM-1 or 10 µM UFP-505 (control; no pretreatment) for 1 h and following a challenge with a range of concentrations of (A) EM-1 or (B) UFP-505. Data are expressed as mean ± SEM (*n* = 5). There were no significant differences in the *pEC*₅₀ of either EM-1 or UFP-505 comparing the pretreatment values with the respective control. Pretreatment *E*_{max} values for both EM-1 and UFP-505 were lower than control; **P* < 0.05; one-way ANOVA with Bonferroni test.

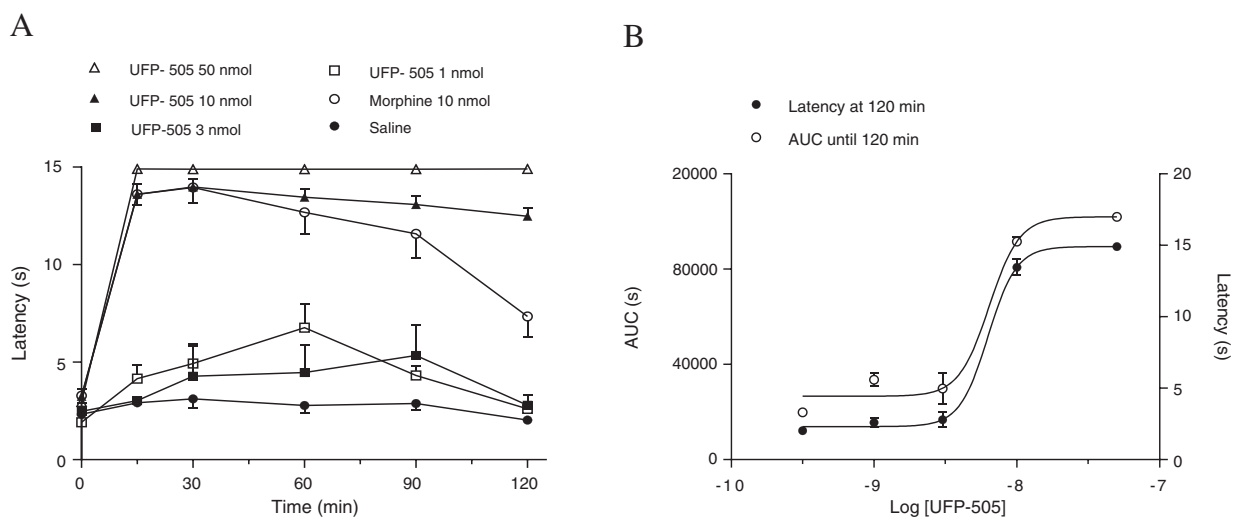


Figure 7

Acute i.t. administration of UFP-505 in the tail flick (TF) nociceptive test. (A) Antinociceptive profile of acute i.t. administration of saline, UFP-505 (1 nmol *n* = 4; 3 nmol, *n* = 7; 10 nmol, *n* = 7; 50 nmol, *n* = 4) and morphine 10 nmol (*n* = 7) in rats using a TF assay (15 s cut-off time). Measurements were taken from 15 to 120 min after a single drug administration. All groups had originally *n* = 8, but due to a technical failure in catheter stabilization, only the animals described here successfully completed the experiments. The antinociception recorded at 120 min after administration for UFP-505 (10 nmol; *n* = 7) was greater than that of morphine (10 nmol). **P* < 0.05, significantly different from saline; #*P*, 0.05, significantly different from morphine; Student's *t*-test. (B) Dose–response curves for UFP-505 produced from the curves in (A), for latency after 120 min of drug administration (expressing antinociception after 2 h) and the corresponding AUC (in s·min, expressing total antinociception). The antinociceptive potency of UFP-505, as deduced from the 120 min latency curve had *pEC*₅₀ 8.20 ± 0.05 (*EC*₅₀ 6.27 nmol), whereas the potency from the AUC curve had *pEC*₅₀ 8.19 ± 0.18 (*EC*₅₀ 6.38 nmol).

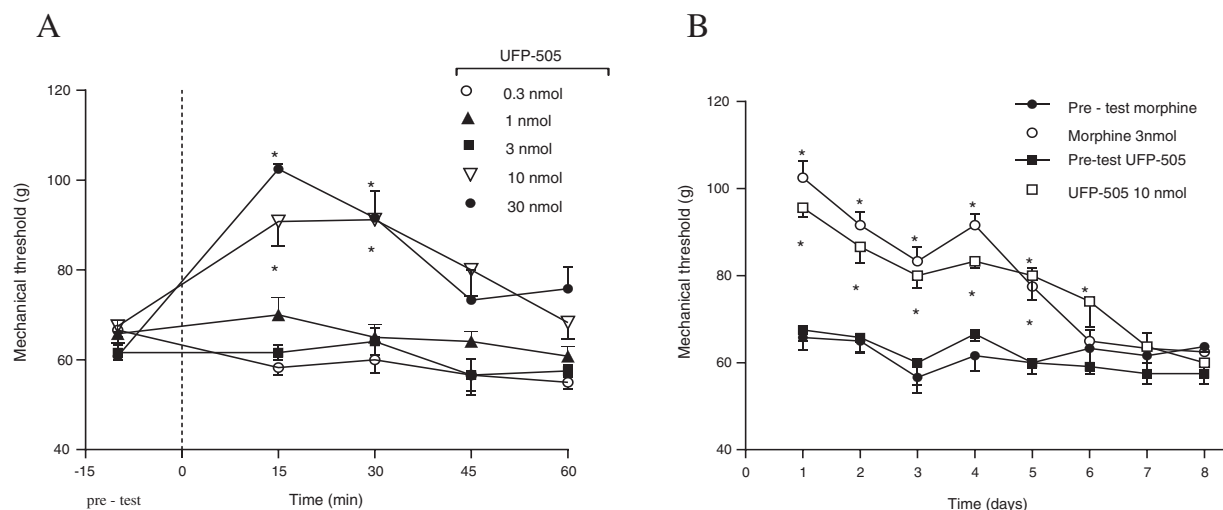


Figure 8

Intrathecal (i.t.) administration of UFP-505 in PP test. (A) Antinociceptive effect of acute i.t. administration of UFP-505 in PP test. The compound was dissolved in saline solution, and a final volume of 10 μ L was administered at the lumbar level of the spinal cord by i.t. catheter. Antinociception was evaluated by PP test. UFP-505 (30 nmol) impaired the locomotor activity of the posterior paws (see Table 1, $*P < 0.05$, compared with pretest values). (B) Antinociceptive effect of repeated i.t. administration of UFP-505 and morphine in a PP test. The compounds were dissolved in saline solution, and a final volume of 10 μ L was administered at the lumbar level of the spinal cord by i.t. catheter. The treatment was repeated daily, and antinociception was evaluated 30 min after administration by PP test. All data are mean \pm SEM; $n = 8$. $*P < 0.05$, significantly different from corresponding pretest values; one-way ANOVA with Bonferroni test.

Table 1

Effect on motor coordination evoked by acute spinal administration of UFP-505

Compound (nmol/i.t.)	Motor coordination (number of falls)				
	Pretest	After treatment (min)			
		15'	30'	45'	60'
UFP-505 0.3	0	0	0	0	0
UFP-505 1	0	0	0	0	0
UFP-505 3	0	0	0	0	0
UFP-505 10	1.0 \pm 0.5	1.0 \pm 0.5	0	0	0
UFP-505 30	0	6 \pm 0	nd	nd	nd

The compound was dissolved in saline solution, and a final volume of 10 μ L was administered at the lumbar level of the spinal cord by i.t. catheter. Motor coordination was evaluated by rotarod test measuring the number of falls in 60 s. The 30 nmol UFP-505 dose impaired locomotor activity of the posterior paws. All data are mean \pm SEM, $n = 8$.

labelling the μ and δ receptors with [3 H]-DAMGO or [3 H]-Nt, in a series of independent binding assays with saturating concentrations of radioligand. Processing of these membranes was based on the same procedures as used for the membranes from cell lysates. Receptor density values (B_{max}) were calculated, and density changes were expressed in % difference from saline-treated animals, as shown in Table 2. Administration of morphine did not induce any changes in receptor density in the frontal cortex for both μ and δ receptors. In contrast, treatment with UFP-505 induced a loss of cell surface μ and δ receptors in this tissue, compared to morphine-treated and untreated membranes. Additionally, for the spinal cord samples, the effect of UFP-505 and morphine on cell surface receptor numbers

was similar (internalization of μ receptors : 44.7%, of δ receptors: 43.1%). A reduction in density of both receptors was observed in the UFP-505-treated samples compared to the expression of the respective receptors in the morphine and untreated samples (Table 1). The ineffectiveness of morphine to internalize the μ receptors agrees with other studies (Whistler and von Zastrow, 1998; Zhang *et al.*, 1998; Bohn *et al.*, 2004) and with the rest of internalization data presented later here.

Additionally, the cortex and spinal cord tissue from treated and non-treated animals were pooled in two discrete groups and processed as two batches to determine opioid receptor mRNA expression by RT-qPCR (expressed as ΔC_t – cycle threshold difference values compared to GAPDH;

Table 2*In vitro* analysis of neuronal tissue taken from i.t.-treated rats

Tissue	Treatment	MOP		DOP	
		B_{max}	Intern. ^a	B_{max}	Intern. ^a
Frontal cortex	Saline	73.85 ± 5.50	–	91.68 ± 8.71	–
	Morphine	71.64 ± 3.51	3%	96.77 ± 3.09	–5.5%
	UFP-505	46.91 ± 1.66	36.5%	40.24 ± 1.31	56.1%
Spinal cord	Saline	23.08 ± 1.94	–	33.12 ± 3.21	–
	Morphine	21.44 ± 0.99	7.1%	32.54 ± 3.85	1.8%
	UFP-505	12.76 ± 2.40	44.7%	18.86 ± 2.08	43.1%

^aInternalization.

Receptor density (B_{max} ; fmol radioligand/mg protein) of MOP and DOP receptors as produced from binding experiments with saturating concentration of radioligand in extensively washed membranes prepared from the frontal cortex and spinal cord tissue, taken from rats treated acutely with either 10 nmol UFP-505 or 10 nmol morphine. Saturation assays were performed using [³H]-DAMGO (≈6.7 nM) and [³H]-NT (≈3.3 nM) respectively. Only the UFP-505-treated animals showed a reduction in both MOP and DOP B_{max} in both tissues. Data are expressed as means ± SEM for $n = 3-4$.

shown in Supporting Information Table S1). In acutely morphine-treated animals, variable changes in opioid receptor mRNA levels were observed for all opioid receptors across all tissues examined. One interesting change that stood out is that acute i.t. morphine and UFP-505-treated animals showed up-regulation of the mRNA for the μ receptors in the spinal cord, but only morphine-treated animals showed simultaneous up-regulation of the δ receptors. The data with morphine align with findings from other studies showing that exposure to morphine increased the surface expression of δ receptors in cultured cortical neurons and in neurons in the dorsal horn of the spinal cord *in vivo* (Cahill *et al.*, 2001; Morinville *et al.*, 2003), although these findings were based on a 48 h exposure to morphine. Furthermore, in the frontal cortex, only the κ receptor mRNA levels were shown to up-regulate in morphine-treated animals. In the rest of the cortex, only the mRNA levels for the δ receptors were significantly down-regulated in both treatment groups. Finally, in the same tissues, levels of the mRNA for the NOP receptor were down-regulated in both treatment groups.

Discussion

Bifunctional opioids have long been studied in opioid pharmacology, either for exploring the relationship between different receptor types or aiming to produce opioid ligands with reduced adverse effects (Dietis *et al.*, 2009; Schiller, 2010). In this study, we show that UFP-505 behaves as a full agonist at the μ receptor and displays a variable expression-dependent efficacy at the δ receptor. This bifunctional compound produces antinociception in rats after i.t. administration.

Partial agonism depends on expression levels

At intermediate levels of expression of δ receptors and in an unamplified system, UFP-505 behaves as a competitive δ receptor antagonist (Dietis *et al.*, 2012), and at very high expression levels in an amplified system, UFP-505 can display a partial agonist activity. This behaviour agrees with

our previous observations that partial agonist behaviour is largely dependent on receptor expression levels (McDonald *et al.*, 2003). Indeed, in CHO_{hDOP} cells, we were able to unmask low efficacy in a GTP γ ³⁵S assay (0.28 relative to DPDPE; unamplified, with δ receptor levels at ~2 pmol·mg⁻¹ protein) and in cAMP assay (amplified, with δ receptor levels at ~1 pmol·mg⁻¹ protein). No activity was shown by UFP-505 in the commercial arrestin assay (unamplified, with δ receptor expression levels unknown) whereas full agonist activity was shown for the loss of cell surface receptors (amplified, with δ receptor levels at ~1 pmol·mg⁻¹ protein).

Reduced radioligand binding translates to true loss of cell surface receptors

The accuracy of receptor expression determined by radioligand labelling is sensitive to 'sticky' ligands that remain bound to receptors, as they may reduce radioligand binding that can be misinterpreted as reduced receptor density. In our standard experimental protocol, we use extensive washing when using natural peptide ligands and radiolabelling (Hashimoto *et al.*, 2002). However, we also constructed a full saturation curve to [³H]DPN in both μ and δ receptor cell lines, in order to provide evidence of effective wash-off, with the resulting K_d of the radioligand being unaffected, indicating that there was no residual desensitizing challenge present at the receptor. We therefore conclude that the reduction in radioligand binding represents a true loss of cell surface receptors. In addition, we show loss of cell surface receptors in well-washed membranes from tissues extracted from whole animals.

Arrestin recruitment and receptor internalization

Control of post-receptor signalling lies in a coordinated interplay between receptor activation and loss of cell surface receptors by endocytosis (internalization). The recruitment of β -arrestin-2 plays a central role to the internalization of opioid receptors and other GPCRs (Zuo, 2005). Early studies showed that morphine fails to internalize the membrane μ receptors (Keith *et al.*, 1996), and stimulation of μ receptor

endocytosis by enhanced β -arrestin-2 can counteract the development of morphine tolerance (Koch *et al.*, 2005). Nevertheless, the involvement of β -arrestin-2 in morphine tolerance is more complicated than a straightforward linear effect, the reduction of cellular levels of β -arrestin-2 may also attenuate morphine tolerance (Yang *et al.*, 2011; Wang *et al.*, 2016). In our assay, activation of μ receptors caused the recruitment of β -arrestin-2 with a rank order of E_{\max} EM1 > fentanyl > UFP-505 > morphine. UFP-505 was able to recruit β -arrestin-2 significantly more than morphine. Despite UFP-505 being a low-efficacy partial agonist at δ receptors and able to induce internalization, the ligand did not show any significant recruitment of β -arrestin-2. We do not know the level of δ receptor expression in this commercial assay, so it is possible that the lack of a partial agonism response by UFP-505 in the δ receptor-expressing cells of this assay could be due to the low receptor expression in this system, unmasked only at higher levels. On the other hand, there are mechanisms of receptor internalization that are independent of β -arrestin-2 (Van Koppen and Jakobs, 2004; Bradbury *et al.*, 2009), and whether these mechanisms are part of UFP-505 activity is unknown. In addition, the ability of a ligand to resensitize μ receptors and to promote recycling is also an important factor for its tolerance profile (Dang and Christie, 2012), an aspect for UFP-505 that needs to be clarified. In essence, UFP-505 was shown to be a ligand unlike morphine in its ability to induce internalization of μ receptors and therefore seemed to have the potential to produce reduced analgesic tolerance compared to morphine.

In vitro studies with a double expression system

We aimed to simulate the *in vivo* situation, where μ and δ receptors are co-expressed, by producing a stable recombinant CHO_{hMOP/DOP} double expression system. In this system, morphine failed to internalize both receptors and UFP-505 was more effective than EM1 in internalizing μ receptors, data that are consistent with the single μ receptor expression system. There was a reduced ability of DPDPE to internalize δ receptors, and while it is tempting to suggest that this may potentially result from the dimer, it could be simply a result of the relatively lower density of δ receptors compared with μ receptors, in this cell line.

The μ and δ receptors have been shown to co-localize *in vivo* (Wang *et al.*, 2005), and their constitutive dimerization plays a functional role in disease and ligand pharmacology (Stockton and Devi, 2012; Yekkirala *et al.*, 2012). Double-expression recombinant systems have been previously used and showed that the potency of opioids may differentiate compared to single-opioid receptor expression cell lines (Yekkirala *et al.*, 2010; Yekkirala *et al.*, 2012). Moreover, the response of these opioids in the μ / δ co-expression system has been shown to be reversed with naltrindole, suggesting a functional interaction between the two receptors. This is in agreement with Waldhoer *et al.* (2005) who showed that heterodimer activation (by 6-guanidinonaltrindole) was tissue-specific and only occurred at the level of the spinal cord. Collectively, these data suggest that δ receptor blockade can reduce the efficacy of morphine when μ receptors are co-expressed, which agrees with the premise of our study that, as δ receptor antagonism reduces morphine tolerance, it may

explain why UFP-505 has reduced tolerance liability. In the longer term, if δ receptor antagonism reduces μ receptor signalling, then it is possible that this could have a 'protective effect' on μ receptors, reducing their ability to desensitize. More importantly, there is evidence to suggest that receptor dimer numbers do change in chronic pain (Costantino *et al.*, 2012), supporting the claims of a vital physiological role of these receptor dimers in disease. Certainly, UFP-505 is able to produce internalization and does not behave like morphine in this respect. In our double-expression system, the potency of UFP-505 is greater by fivefold than in the single μ receptor expression system, suggesting that our bifunctional ligand is interacting with a functional μ - δ receptor heterodimer. Clearly, further experimentation with tagged opioid receptors and UFP-505 are required.

In vivo experiments

Acute i.t. injection of UFP-505 produced a robust antinociceptive response in the TF assay with potency (ED_{50}) of ~7 nmol and 10 nmol of UFP-505 was as antinociceptive as 10 nmol of morphine. More importantly, our data show that UFP-505 produced prolonged antinociception that persisted more than 120 min after acute administration, compared with the time course of morphine antinociception. Similar data were obtained in the PP test (using a different catheterization strategy) with ED_{50} for UFP-505 of ~9 nmol. These data confirm for the first time the presumption of a strong antinociceptive dose-dependent effect of UFP-505 as a μ receptor ligand with agonist activity. Morphine tolerance has been consistently observed in rats after 3 days with i.t. treatment (Granados-Soto *et al.*, 2000; Paul *et al.*, 2017) or 5 days with s.c (Goodchild *et al.*, 2009) or i.p treatment (Chen *et al.*, 2008). We confirmed these findings for morphine with our long-term testing using the PP test. Bifunctional ligands with a μ receptor agonist and δ receptor antagonist profile have been shown to have reduced tolerance profile (Mosberg *et al.*, 2014), and therefore, we expected that UFP-505 would show a similar profile in our long-term tests of paw withdrawal, given its pharmacological profile *in vitro* and its analgesic efficacy *in vivo*. However, to our surprise, UFP-505 produced a tolerance profile that was not significantly different from that of morphine in our model.

Although we have no data that will offer a mechanistic explanation of UFP-505's tolerance profile, there are two factors that could explain this unexpected result. The first is the model in which antinociception is assessed. Different pain models, such as TF, hot-plate, PP, warm water tail-withdrawal, capsaicin administration and acetic acid writhing) utilize different types of nociceptive stimuli (electrical, thermal, mechanical and chemical) that require the involvement of a mixed variety of neuronal processes (Le Bars *et al.*, 2001). Given the complex molecular changes that occur during long-term exposure of opioids and the stimuli differences between antinociceptive models, it is possible that the development of nociceptive tolerance is model-sensitive. Another potential contributor to the tolerance profile of UFP-505 is the dose and method of administration used. Some recent studies have suggested a dose dependence for the induction of opioid tolerance (Pawar

et al., 2007; Madia *et al.*, 2009), which increases the difficulty of efficiently comparing data from studies that use different opioid doses and routes of administration. A simpler explanation could be that the observed residual agonist activity at δ receptors may become important in producing tolerance. Studies with a *pure* δ receptor antagonist would help to settle this point.

Nevertheless, the profile of tolerance liability in opioids that possess a bi- or multi-functional activity profile is not new. A characteristic example of such a ligand is buprenorphine, a well-known and fully characterized complex opioid that has been studied for more than 40 years (Lutfy and Cowan, 2004). Although buprenorphine is a μ receptor partial agonist, and an antagonist at δ and κ receptors (Huang *et al.*, 2001), its tolerance profile is somewhat similar to morphine (Paronis and Bergman, 2011). Nevertheless, the pharmacokinetic profile and a lack of a ceiling effect in the clinical setting are seen as an advantage (Louis, 2006; Khanna and Pillarisetti, 2015).

The main aim of the study was to fully characterize a promising bifunctional ligand (based on earlier data) and to provide insights on the potential relationship between *in vitro* and *in vivo* activity. Full characterization of a bifunctional opioid with multiple *in vitro/ex vivo/in vivo* assays is important but not often performed. Our data present a continuum from basic pharmacology to antinociceptive actions *in vivo*. Specifically, this study of UFP-505 (*in vitro* and *in vivo*) offers invaluable information on the pharmacological properties that bifunctional opioids may present. Unfortunately, the lack of antinociceptive efficacy of UFP-505 via an additional subcutaneous route (see Supporting Information Figure S1) may preclude further development. Nevertheless, the insights gained from studying UFP-505 are of value in the search for newer opioid-like compounds with increased antinociceptive efficacy and reduced liability for tolerance.

Acknowledgements

This work has been supported by HOPE Against Cancer (www.hfcr.org). N.D. was the recipient of the British Pharmacological Society Schachter Award (www.bps.ac.uk). We would like to thank Dr David Lodwick and Sonja Khemiri for their help with the novel cell line production and Prof T Costa for his constructive advice on receptor internalization.

Author contributions

D.G.L., G.C., R.G., S.S., D.J.R. and N.D. are involved in the planning and design of the study. N.D. collected or coordinated the collection of all data. H.N., R.T. and J.Mc.D. were involved in collection of *in vitro* data in Leicester. V.R., M.F., G.V. and N.D. collected *in vivo* data in Modena, Italy. L.M. and C.G. collected *in vivo* data in Florence, Italy. All authors were involved in interpretation of the data and approved the final draft of the manuscript. H.N. and R.T. contributed equally to this work.

Conflict of interest

R.G. S.S. and G.C. are members of a University spin-out company, University of Ferrara Peptides (UFPeptides), which is involved in the development of opioid ligands. Other listed authors are collaborators with UFPeptides. UFP-505 is not subject to patent and may be made available on request to RG/SS.

Declaration of transparency and scientific rigour

This Declaration acknowledges that this paper adheres to the principles for transparent reporting and scientific rigour of preclinical research recommended by funding agencies, publishers and other organisations engaged with supporting research.

References

- Abdelhamid EE, Sultana M, Portoghese PS, Takemori AE (1991). Selective blockage of delta opioid receptors prevents the development of morphine tolerance and dependence in mice. *J Pharmacol Exp Ther* 258: 299–303.
- Alexander SPH, Christopoulos A, Davenport AP, Kelly E, Marrion NV, Peters JA *et al.* (2017). The Concise Guide to PHARMACOLOGY 2017/18: G protein-coupled receptors. *Br J Pharmacol* 174 (Suppl 1): S17–S129.
- Balbani G, Salvadori S, Trapella C, Knapp BI, Bidlack JM, Lazarus LH *et al.* (2010). Evolution of the bifunctional lead μ agonist / δ antagonist containing the DMT-TIC opioid pharmacophore. *ACS Chem Neurosci* 1: 155–164.
- Bohn LM, Dykstra LA, Lefkowitz RJ, Caron MG, Barak LS (2004). Relative opioid efficacy is determined by the complements of the G protein-coupled receptor desensitization machinery. *Mol Pharmacol* 66: 106–112.
- Bradbury FA, Zelnik JC, Traynor JRG (2009). Protein independent phosphorylation and internalization of the δ -opioid receptor. *J Neurochem* 109: 1526–1535.
- Cahill CM, Morinville A, Lee MC, Vincent JP, Collier B, Beaudet A (2001). Prolonged morphine treatment targets delta opioid receptors to neuronal plasma membranes and enhances delta-mediated antinociception. *J Neurosci* 21: 7598–7607.
- Chen TC, Cheng YY, Sun WZ, Shyu BC (2008). Differential regulation of morphine antinociceptive effects by endogenous enkephalinergic system in the forebrain of mice. *Mol Pain* 4: 41.
- Cheng Y, Prusoff WH (1973). Relationship between the inhibition constant (K₁) and the concentration of inhibitor which causes 50 per cent inhibition (I₅₀) of an enzymatic reaction. *Biochem Pharmacol* 22: 3099–3108.
- Costantino CM, Gomes I, Stockton SD, Lim MP, Devi LA (2012). Opioid receptor heteromers in analgesia. *Expert Rev Mol Med* 14: e9.
- Curtis MJ, Bond RA, Spina D, Ahluwalia A, Alexander SP, Giembycz MA *et al.* (2015). Experimental design and analysis and their reporting: new guidance for publication in BJP. *Br J Pharmacol* 172: 3461–3471.

- Dang VC, Christie MJ (2012). Mechanisms of rapid opioid receptor desensitization, resensitization and tolerance in brain neurons. *Br J Pharmacol* 165: 1704–1716.
- Dietis N, Guerrini R, Calo G, Salvadori S, Rowbotham JD, Lambert GD (2009). Simultaneous targeting of multiple opioid receptors. A strategy to improve side effect profile. *Br J Anaesth* 103: 38–49.
- Dietis N, McDonald J, Molinari S, Calo G, Guerrini R, Rowbotham JD *et al.* (2012). Pharmacological characterisation of the bifunctional opioid ligand H-Dmt-Tic-Gly-NH-Bzl (UFP-505). *Br J Anaesth* 108: 262–270.
- Dietis N, Rowbotham JD, Lambert GD (2011). Controlling cancer pain: Is morphine the best we can do? *Trends in Anaesthesia and Critical Care* 1: 227–229.
- George SR, Fan T, Xie Z, Tse R, Tam V, Varghese G *et al.* (2000). Oligomerization of mu and delta-opioid receptors. Generation of novel functional properties. *J Biol Chem* 275: 26128–26135.
- Gomes I, Jordan BA, Gupta A, Trapaidze N, Nagy V, Devi LA (2000). Heterodimerization of mu and delta opioid receptors: a role in opiate synergy. *J Neurosci* 20: RC110.
- Goodchild CS, Kolosov A, Geng L, Winter LL, Nadeson R (2009). Prevention and reversal of morphine tolerance by the analgesic neuroactive steroid alphadolone. *Pain Med* 10: 890–901.
- Granados-Soto V, Kalcheva I, Hua X, Newton A, Yaksh TL (2000). Spinal PKC activity and expression: role in tolerance produced by continuous spinal morphine infusion. *Pain* 85: 395–404.
- Gupta A, Décaillot FM, Devi LA (2006). Targeting opioid receptor heterodimers: strategies for screening and drug development. *AAPS J* 8: E153–E159.
- Harding SD, Sharman JL, Faccenda E, Southan C, Pawson AJ, Ireland S *et al.* (2018). The IUPHAR/BPS Guide to PHARMACOLOGY in 2018: updates and expansion to encompass the new guide to IMMUNOPHARMACOLOGY. *Nucl Acids Res* 46: D1091–D1106.
- Hashimoto Y, Calo G, Guerrini R, Smith G, Lambert DG (2002). Effects of chronic nociceptin/orphanin FQ exposure on cAMP accumulation and receptor density in Chinese hamster ovary cells expressing human nociceptin/orphanin FQ receptors. *Eur J Pharmacol* 449: 17–22.
- Hepburn MJ, Little PJ, Gingras J, Kuhn CM (1997). Differential effects of naltrindole on morphine-induced tolerance and physical dependence in rats. *J Pharmacol Exp Ther* 281: 1350–1356.
- Huang P, Kehner GB, Cowan A, Liu-Chen LY (2001). Comparison of pharmacological activities of buprenorphine and norbuprenorphine: norbuprenorphine is a potent opioid agonist. *J Pharmacol Exp Ther* 297: 688–695.
- Keith DE, Murray SR, Zaki PA, Chu PC, Lissin DV, Kang L *et al.* (1996). Morphine activates opioid receptors without causing their rapid internalization. *J Biol Chem* 271: 19021–19024.
- Kest B, Lee CE, McLemore GL, Inturrisi CE (1996). An antisense oligodeoxynucleotide to the delta opioid receptor (DOR-1) inhibits morphine tolerance and acute dependence in mice. *Brain Res Bull* 39: 185–188.
- Khanna K, Pillarisetti S (2015). Buprenorphine – an attractive opioid with underutilized potential in treatment of chronic pain. *J Pain Res* 8: 859–870.
- Kilkenny C, Browne W, Cuthill IC, Emerson M, Altman DG (2010). NC3Rs reporting guidelines working group. *Br J Pharmacol* 160: 1577–1579.
- Kitayama M, McDonald J, Barnes TA, Calo G, Guerrini R, Rowbotham DJ *et al.* (2007). In vitro pharmacological characterisation of a novel cyclic nociceptin/orphanin FQ analogue c[Cys(7,10)]N/OFQ(1-13)NH(2). *Naunyn Schmiedeberg Arch Pharmacol* 375: 369–376.
- Koch T, Wiedera A, Bartzsch K, Schulz S, Brandenburg LO, Wundrack N *et al.* (2005). Receptor endocytosis counteracts the development of opioid tolerance. *Mol Pharmacol* 67: 280–287.
- Lambert DG (2008). The nociceptin/orphanin FQ receptor: a target with broad therapeutic potential. *Nat Rev Drug Discov* 7: 694–710.
- Law PY, Erickson-Herbrandson LJ, Zha QQ, Solberg J, Chu J, Sarre A *et al.* (2005). Heterodimerization of mu- and delta-opioid receptors occurs at the cell surface only and requires receptor-G protein interactions. *J Biol Chem* 280: 11152–11164.
- Le Bars D, Gozariu M, Cadden SW (2001). Animal models of nociception. *Pharmacol Rev* 53: 597–652.
- Leighton GE, Rodriguez RE, Hill RG, Hughes J (1988). k-opioid agonist produce antinociception after i.v. and i.c.v. but not intrathecal administration in the rat. *Br J Pharmacol* 93: 553–560.
- Louis F (2006). Transdermal buprenorphine in pain management – experiences from clinical practice: five case studies. *Int J Clin Pract* 60: 1330–1334.
- Lutfy K, Cowan A (2004). Buprenorphine: a unique drug with complex pharmacology. *Curr Neuropharmacol* 2: 395–402.
- Madia PA, Dighe SV, Sirohi S, Walker EA, Yoburn BC (2009). Dosing protocol and analgesic efficacy determine opioid tolerance in the mouse. *Psychopharmacology (Berl)* 207: 413–422.
- McDonald J, Barnes TA, Okawa H, Williams J, Calo G, Rowbotham DJ *et al.* (2003). Partial agonist behaviour depends upon the level of nociceptin/orphanin FQ receptor expression: studies using the ecdysone-inducible mammalian expression system. *Br J Pharmacol* 140: 61–70.
- McGrath JC, Lilley E (2015). Implementing guidelines on reporting research using animals (ARRIVE etc.): new requirements for publication in BJP. *Br J Pharmacol* 172: 3189–3193.
- Micheli L, Di Cesare Mannelli L, Guerrini R, Trapella C, Zanardelli M, Ciccocioppo R *et al.* (2015). Acute and subchronic antinociceptive effects of nociceptin/orphanin FQ receptor agonists infused by intrathecal route in rats. *Eur J Pharmacol* 754: 73–81.
- Morinville A, Cahill CM, Esdaile MJ, Aibak H, Collier B, Kieffer BL *et al.* (2003). Regulation of delta-opioid receptor trafficking via mu-opioid receptor stimulation: evidence from mu-opioid receptor knock-out mice. *J Neurosci* 23: 4888–4898.
- Mosberg HI, Yeomans L, Anand JP, Porter V, Sobczyk-Kojiro K, Traynor JR *et al.* (2014). Development of a bioavailable μ opioid receptor (MOPr) agonist, δ opioid receptor (DOPr) antagonist peptide that evokes antinociception without development of acute tolerance. *J Med Chem* 57: 3148–3153.
- Nitsche JF, Schuller AG, King MA, Zengh M, Pasternak GW, Pintar JE (2002). Genetic dissociation of opiate tolerance and physical dependence in delta-opioid receptor-1 and preproenkephalin knock-out mice. *J Neurosci* 22: 10906–10913.
- Paronis C, Bergman J (2011). Buprenorphine and opioid antagonism, tolerance, and naltrexone-precipitated withdrawal. *J Pharmacol Exp Ther* 336: 488–495.
- Paul AK, Gueven N, Dietis N (2017). Morphine dosing strategy plays a key role in the generation and duration of the produced antinociceptive tolerance. *Neuropharmacology* 121: 158–166.

- Pawar M, Kumar P, Sunkaraneni S, Sirohi S, Walker EA, Yoburn BC (2007). Opioid agonist efficacy predicts the magnitude of tolerance and the regulation of mu-opioid receptors and dynamin-2. *Eur J Pharmacol* 563: 92–101.
- Schiller PW (2010). Bi- or multifunctional opioid peptide drugs. *Life Sci* 86: 598–603.
- Sehgal N, Colson J, Smith HS (2013). Chronic pain treatment with opioid analgesics: benefits versus harms of long-term therapy. *Expert Rev Neurother* 13: 1201–1220.
- Stockton SD, Devi LA (2012). Functional relevance of μ - δ opioid receptor heteromerization: a role in novel signaling and implications for the treatment of addiction disorders: from a symposium on new concepts in mu-opioid pharmacology. *Drug Alcohol Depend* 121: 167–172.
- Storkson RV, Kjorsvik A, Tjolsen A, Hole K (1996). Lumbar catheterization of the spinal subarachnoid space in the rat. *J Neurosci Methods* 65: 167–172.
- Toll L, Caló G, Cox BM, Chavkin C, Christie MJ, Civelli O *et al.* (2018). Opioid receptors. Accessed on 07/03/2018. IUPHAR/BPS Guide to PHARMACOLOGY. Available at <http://www.guidetopharmacology.org/GRAC/FamilyDisplayForward?familyId=50>.
- Van Koppen CJ, Jakobs KH (2004). Arrestin-independent internalization of G protein-coupled receptors. *Mol Pharmacol* 66: 365–367.
- Waldhoer M, Fong J, Jones RM, Lunzer MM, Sharma SK, Kostenis E *et al.* (2005). A heterodimer-selective agonist shows in vivo relevance of G protein-coupled receptor dimers. *Proc Natl Acad Sci U S A* 102: 9050–9055.
- Wang D, Sun X, Bohn LM, Sadée W (2005). Opioid receptor homo- and heterodimerization in living cells by quantitative bioluminescence resonance energy transfer. *Mol Pharmacol* 67: 2173–2184.
- Wang J, Xu W, Zhong T, Song Z, Zou Y, Ding Z *et al.* (2016). miR-365 targets β -arrestin 2 to reverse morphine tolerance in rats. *Sci Rep* 6: 38285.
- Whistler JL, von Zastrow M (1998). Morphine-activated opioid receptors elude desensitization by arrestin. *Proc Natl Acad Sci U S A* 95: 9914–9919.
- Williams J, Ingram S, Henderson G, Chavkin C, Von Zastrow M, Schulz S *et al.* (2013). Regulation of μ -opioid receptors: desensitization, phosphorylation, internalization, and tolerance. *Pharmacol Rev* 65: 223–254.
- Yaksh TL, Rudy TA (1976). Chronic catheterization of the spinal subarachnoid space. *Physiol Behav* 17: 1013–1016.
- Yang CH, Huang HW, Chen KH, Chen YS, Sheen-Chen SM, Lin CR (2011). Antinociceptive potentiation and attenuation of tolerance by intrathecal-arrestin 2 small interfering RNA in rats. *Brit J Anaesth* 107: 774–781.
- Yekkirala AS, Banks ML, Lunzer MM, Negus SS, Rice KC, Portoghese PS (2012). Clinically employed opioid analgesics produce antinociception via μ - δ opioid receptor heteromers in Rhesus monkeys. *ACS Chem Neurosci* 3: 720–727.
- Yekkirala AS, Kalyuzhny AE, Portoghese PS (2010). Standard opioid agonists activate heteromeric opioid receptors: evidence for morphine and [d-Ala(2)-MePhe(4)-Glyol(5)]enkephalin as selective μ -d agonists. *ACS Chem Neurosci* 1: 146–154.
- Zhang J, Ferguson SS, Barak LS, Bodduluri SR, Laporte SA, Law PY *et al.* (1998). Role for G protein-coupled receptor kinase in agonist-specific regulation of mu-opioid receptor responsiveness. *Proc Natl Acad Sci U S A* 95: 7157–7162.
- Zhu Y, King MA, Schuller AG, Nitsche JF, Reidl M, Elde RP *et al.* (1999). Retention of supraspinal delta-like analgesia and loss of morphine tolerance in delta opioid receptor knockout mice. *Neuron* 24: 243–252.
- Zuo Z (2005). The role of opioid receptor internalization and beta-arrestins in the development of opioid tolerance. *Anesth Analg* 101: 728–734, table of contents.

Supporting Information

Additional Supporting Information may be found online in the supporting information tab for this article.

<https://doi.org/10.1111/bph.14199>

Table S1 Opioid receptor mRNA expression changes in neural tissue from treated rats.

Figure S1 Tail-withdrawal assay. Morphine was dissolved in saline whilst UFP-505 was dissolved in 1% DMSO and 100 μ L/mouse was administered subcutaneously at 30 min before the test to CD1 male mice (25–30 g). Antinociception was evaluated by tail-withdrawal assay in a water temperature of 48°C and cut off time 20 s. Data are mean + SEM, 4 animals in each group.